Instantaneous mechanical fastening of quasi-isotropic CFRP laminates by a self-piercing rivet

Masahito Ueda [a,*], Sotaro Miyake [a], Hiroyuki Hasegawa [b], Yoshiyasu Hirano [c]

[a] Nihon University

  1-8-14 Kanda-surugadai, Chiyoda, Tokyo 101-8308, Japan

  E-mail: ueda@mech.cst.nihon-u.ac.jp

  Tel & Fax: +81-3-3259-0746

[b] Fukui Byora Co., Ltd.

  3-2-2 Higashi-Machi, Daishoji, Kaga, Ishikawa 922-0816, Japan

[c] Japan aerospace exploration agency

  6-13-1 Oosawa, Mitaka, Tokyo 181-0015, Japan

*Corresponding author

ABSTRACT

A modified self-piercing rivet (SPR) has been proposed to mechanically fasten CFRP laminates. The modified SPR consists of a rivet body and two flat washers. The two flat washers were used to suppress delamination in the CFRP laminates at the point of piercing. The advantages of the modified SPR for fastening CFRP laminates are instantaneous process time and low cost. Any pretreatments such as surface treatments or hole drilling are not required. In this study, the viability of the modified SPR for a quasi-isotropic CFRP laminate was investigated by tensile and fatigue tests on the single lap joints. The experimental results showed that the tensile strength of a modified SPR joint was slightly higher than a bolted joint. In tension-tension fatigue tests, a fatigue limit at $N_f=10^7$ cycles was about 50 % of the tensile joint strength. Experimental results showed that the modified SPR was one of the promising fasteners for future mass-production CFRP automobiles.

Keywords: CFRP, Joint, Fastener, Strength, Fatigue

1. Introduction

Because of the strong demand for weight reduction in mass produced automobiles, structural steel components are progressively being replaced by carbon fiber reinforced plastic (CFRP) laminates. Spot welding is in general use in steel structures as a low cost and instantaneous joint. There is, however, no such instantaneous joining technique for CFRP laminates, which is inhibiting the wide application of CFRP laminates in automotive structures.

Adhesive is generally used to fasten CFRP laminates. However, this is a problem for mass production. Lengthy times are required for curing and additional surface treatment, which increase manufacturing cost. The effects of temperature, humidity and strain rate on the mechanical properties need careful consideration [1-3].

Mechanical fasteners such as rivets or bolts are also used to fasten CFRP laminates [4]. This, however, requires hole drilling before fastening, which takes time and requires care to prevent damage in the CFRP laminates [5, 6]. Tool life becomes shorter for CFRP laminates than for steel fabrication [7]. Therefore, low cost and instant fasteners for CFRP laminates are required to resolve the problems of the adhesives and the conventional rivet or bolt fasteners.

A self-piercing rivet (SPR) has been adopted to fasten metal sheets [8, 9]. Hole drilling is unnecessary in the fastening process, which drastically reduces processing time. However, there are no reports on the fastening of the CFRP laminates by SPRs since they may easily cause damage such as delamination at the points of piercing. In this study, a modified SPR is proposed to minimize delamination at the points of piercing. Instantaneous mechanical fastening of quasi-isotropic CFRP laminates was performed using the modified SPR. The viability of the modified SPR for CFRP laminates was discussed from the experimental results of quasi-static tensile and fatigue tests on single lap joints.

2. Modified SPR

2.1 Materials and configuration

Fig. 1 shows the configuration of a modified SPR. The modified SPR consists of a rivet body and two flat washers. Materials of the rivet body and the flat washers are SCM435 and S45C respectively. SCM435 was used because it has been in use for the conventional SPR on metal sheets. The corrosion problem between the rivet body and a CFRP needs to be resolved by surface coating or by changing the material of the rivet body, which is beyond the scope of this study.

2.2 Fastening process

Since the rivet body pierces the CFRP laminates in the fastening process, initial hole drilling is not required. However, damage to the CFRP laminates such as delamination due to the piercing process needs to be suppressed because it propagates under fatigue load, which drastically reduces the acceptable mechanical properties of CFRP laminates. In fastening using the modified SPR, delamination is suppressed by applying pressure to the CFRP laminates during piercing.

Figs. 2a and 2b show cross-sectional drawings of CFRP laminates before fastening (before piercing) and after fastening (after piercing). The upper and lower flat washers (1) and (2) are placed on the upper and lower supporting dies (3) and (4). After positioning the supporting dies at a fastening point, the upper and lower supporting dies are pressed against the CFRP laminates. Since the pressure needs to be applied very close to the piercing hole to prevent delamination, two flat washers were used. Therefore, pressure was applied by the two supporting dies through the two flat washers. Maintaining the pressure, the rivet body pierced the CFRP laminates. Chopped CFRP at the rivet body due to the piercing was discharged through the lower supporting die. After piercing, the cutting tip of the rivet body was curled by the lower supporting die, to complete the fastening process. Fastening using the modified SPR requires no initial hole drilling which enables instant fastening by means of an automatic riveting machine.

The clearance between the outer diameter of the rivet body and inner diameter of the washers affects the suppression of delamination in the piercing process. There is a curvature (of radius R) at the neck part of the rivet

body to reduce stress concentration (see Fig. 1a). For the upper flat washer, the chamfer (of length C_1) was machined at the inner corner (see Fig. 1b). The chamfered length is slightly larger than the curvature radius on the rivet, by which the clearance between the outer diameter of the rivet body and the inner diameter of the upper flat washers was minimized. For the lower flat washer, the inner diameter should be almost the same as the outer diameter of the rivet body although this depends on the positioning accuracy and stiffness of the rivet body. In this study, 5.0 mm for the outer diameter of the rivet body and 5.1 mm for the inner diameter of the flat washers were selected. The diameter and thickness of the rivet body should be properly selected according to CFRP laminates to prevent bucking of the rivet body in the piercing process.

In this study, the fastening process was divided into two steps to measure the applied load to the CFRP laminates. First step was a piercing process of the CFRP laminates by the rivet body. Second step was a swaging process of the cutting tip. Both processes were performed using a riveting machine under control of displacement.

Figs. 3a and 3b show load-time curves in the piercing and swaging process. The upper and lower supporting dies were pressed against the CFRP laminates at 6.5 kN. Maximum load in the piercing process was about 18 kN which included 6.5kN pre-loading by the supporting dies. Then, swaging of the cutting tip was performed. Maximum load in the swaging process was 38 kN. The load in the thickness direction has been applying to the CFRP laminates by the rivet body through the flat washers after the fastening.

2.3 Damages in CFRP laminate due to piercing

Fig. 4a shows a cross-sectional photograph of quasi-isotropic CFRP laminates after fastening using the modified SPR. Fig. 4b shows schematic drawing of Fig. 4a. The material and stacking sequence of the CFRP laminates are shown in Section 3.1. Dragging of the plies due to the piercing was found around the piercing hole. Delamination was not apparent using visual inspection because the delaminated plies were clamped together by the modified SPR. It may be impossible topologically to drag the plies without separation of the plies, which indicates delamination in the dragging area.

The modified SPR was removed after the fastening to measure the delamination size. The delamination in the CFRP laminates was measured by means of ultrasonic inspection (SDS-5400R, Krautkramer). Fig. 5 shows C-scan images of the delamination in the CFRP laminates and the external appearances. The size of the delamination due to the piercing was much smaller than the diameter of the flat washer. Delamination can be adequately suppressed by applying pressure to the CFRP laminates in the piercing process.

3. Material and specimen configuration

3.1 CFRP laminate

Quasi-isotropic CFRP laminates were made using a unidirectional prepreg tape in the autoclave molding method. The prepreg tape used in this study was T800SC/#2592 produced by Toray Industries. The stacking sequence was $[45_2/0_2/-45_2/90_2]$s. After curing the CFRP laminates, it was cut into a rectangular shape of 135 mm long and 36 mm wide using a diamond cutting machine. The thickness of the laminate was 1.6 mm. The fiber volume fraction was about 65 %.

3.2 Single lap joint

The configuration of a single lap joint for quasi-static tensile and fatigue tests is shown in Fig. 6, which was followed by ASTM D5961 except the thickness. A bolted joint with the same configuration was also prepared to compare the joint strengths. For the bolted joint, initially a 5.1 mm hole was drilled and the laminates were then jointed using an M5 bolt and nut. The material of the bolt was SCM435. The bolt had a smoothed circular cylinder part which was in contact with the hole through the CFRP laminates. The bolt and nut were tightened using only fingers so that pressure was not applied to the CFRP laminates. The washers used for the modified SPR joint were also used for the bolted joint.

4. Quasi-static tensile test

4.1 Experimental procedure

Quasi-static tensile tests of the single lap joints were performed using a universal testing machine (AG-IS150kN, Shimadzu). Crosshead speed was 1.0 mm/min.

4.2 Results and discussion

Fig. 7 shows the load-displacement curves of the two single lap joints made by a modified SPR and a bolt. The tensile tests were performed three times for each joint, in which almost the same load-displacement curves were obtained. The joint stiffness was relatively higher for the modified SPR joint than for the bolted joint. The average maximum loads P_U in the three tests were 8.0 kN for the modified SPR joint and 7.2 kN for the bolted joint. A slightly higher maximum load was observed for the modified SPR joint than for the bolted joint. Clearance between the fastener and the hole was smaller for the modified SPR joint than the bolted joint since the modified SPR pierces into the CFRP laminate without drilling. The contact area was, therefore, larger for the modified SPR joint, which increased the joint stiffness and the joint strength [10]. Load was suddenly dropped for the bolted joint just after reaching maximum load. By contrast, the maximum load for the modified SPR joint was retained for a period of time. The load in the thickness direction was applied to the CFRP laminates by the rivet body because of the swaging process of the cutting tip. The relatively high constraint in the thickness direction prevented catastrophic failure of the CFRP laminates, enabling the modified SPR joint to retain the maximum load for a period of time [11-13].

Fig. 8 shows the external appearance of the single lap joints after tensile tests. The tensile tests were continued until the joints separated. The failure mode was bearing failure for both joints as shown in Fig. 9a. Fig. 9b shows damage progress of the bearing failure. Since the thickness was relatively thin, the rivet body was pulled out from the CFRP laminate as a result of the bearing failure. Previous studies indicate bearing failure for the specimen configuration [13, 14].

5 Fatigue test

5.1 Experimental procedure

Fatigue tests on the single lap joints were performed by a hydraulic fatigue testing machine (8802, Instron). The stress ratio was fixed to $R=0.1$. The maximum load P_{max} was changed to 90, 80, 70, 60, 55, 50, 40 % of the static tensile strength P_U. The test frequency was 2 Hz. Fatigue tests were performed only for the modified SPR jointed CFRP laminates.

5.2 Results and discussion

The relationship of the maximum load and number of cycles to failure is shown in Fig. 10. The rectangular plot indicates failure of the CFRP laminates and the circular plot indicates failure of the rivet body. The CFRP laminates failed when $P_{\max} \geqq 0.8 P_{\mathrm{U}}$. By contrast, the rivet body failed before the CFRP laminates when $0.55 P_{\mathrm{U}} \leqq P_{\max} \leqq 0.8 P_{\mathrm{U}}$. Both failures were randomly observed when $P_{\max} = 0.8 P_{\mathrm{U}}$. The fatigue limit was $0.5 P_{\mathrm{U}}$ if the maximum number of cycles was limited to $N_{\mathrm{f}} = 10^7$.

In the case of rivet body failure, a crack developed at the curled part of the rivet body. The crack then progressed and deformation of the curled part increased with the increase in the number of cycles. The curled part then failed. The single lap joint was bent because of the tensile load, which developed stress concentrations at the curled and neck parts of the rivet body. Since the curled part was already damaged due to plastic deformation in the swaging process, it failed before the neck part. When the maximum load was less than 80 % of the static tensile joint strength, the fatigue strength of the modified SPR jointed CFRP laminates was determined by the fatigue strength of the rivet body under this condition. The fatigue strength of the modified SPR joint can be improved by changing the configuration of the cutting tip and swaging condition.

In the case of CFRP laminate failure, the failure mode was bearing failure.

5.3 Delamination after fatigue test

Fig. 11 shows the external appearance of the modified SPR jointed CFRP laminates after $N_{\mathrm{f}} = 10^7$ cycles when the maximum load was $0.5 P_{\mathrm{U}}$, i.e., the fatigue limit. No visible damage was observed from the external appearance of the CFRP laminates.

The rivet body was then removed from the CFRP laminates to take C-scan images of the delamination around the hole. Fig. 12 shows the C-scan images of delamination around the hole. Delamination progressed around the piercing hole compared to that just before piercing (see Fig. 5). The size of the delamination was still smaller than the outer diameter of the washer.

Delamination in the lower laminate (curled side) at the point of piercing was greater than in the upper laminate (pierced side). After the fatigue test, delamination in the lower laminate was still greater than in the upper laminate. Since the delamination at the point of piercing originated during the progress of the fatigue loading, delamination needs to be suppressed as thoroughly as possible in the fastening process.

Fig. 13 shows C-scan images of delamination in modified SPR jointed CFRP laminates after $N_{\mathrm{f}} = 10^7$ cycles when the maximum load was $0.4 P_{\mathrm{U}}$. In this case, progress of the delamination was reduced.

6. Conclusions

A modified SPR was proposed to instantly fasten CFRP laminates. The viability of the newly developed mechanical fastener was investigated using quasi-isotropic CFRP laminates made by a prepreg tape. Quasi-static tensile and fatigue tests of the single lap joints were performed. The results obtained in this paper are summarized as follows.

1. Pressure was applied to the CFRP laminates by two supporting dies through two flat washers during the piercing process. Delamination was sufficiently suppressed by minimizing the clearance between the outer

diameter of the rivet body and inner diameter of the washers. The CFRP laminates were mechanically fastened instantaneously without the need to drill a hole.

2. The modified SPR joint showed greater joint stiffness and strength than the bolted joint. The maximum load was retained for a period of time for the modified SPR joint although the load was suddenly dropped for the bolted joint. The failure mode of the joints was bearing failure.

3. The fatigue limit of the modified SPR jointed CFRP laminates was 50 % of the static tensile joint strength. The rivet body failed prior to the CFRP laminates when the maximum load was lower than 80 % of the static tensile joint strength. By contrast, the CFRP laminates failed prior to the rivet body when the maximum load was higher than 80 % of the static tensile joint strength.

4. Delamination in the modified SPR jointed CFRP laminates after the fatigue test of 10^7 cycles was smaller than the diameter of the washer when the maximum load was less than 50 % of the tensile joint strength.

References

1. Ashcroft IA, Hughes DJ, Shaw SJ, Wahab MA, Crocombe A. Effect of temperature on the quasi-static strength and fatigue resistance of bonded composite double lap joints. Journal of adhesives 2001; 75(1): 61-68.

2. Ferreira JAM, Reis PN, Costa JDM, Richardson MOW. Fatigue behaviour of composite adhesive lap joints. Composites Science and Technology 2002; 62(10-11): 1373-1379.

3. Casas-Rodriguez J.P, Ashcroft I.A, Silberschmidt V.V. Damage in adhesively bonded CFRP joints: Sinusoidal and impact-fatigue. Composites Science and Technology 2008; 68(13):2663-2670.

4. Thoppul S. D, Finegan J, Gibson R.F. Mechanics of mechanically fastened joints in polymer–matrix composite structures – A review. Composites Science and Technology 2009; 69(3-4): 301-329.

5. Khashaba U.A, El-Sonbaty I.A, Selmy A.I, Megahed A.A. Machinability analysis in drilling woven GFR/epoxy composites: Part I – Effect of machining parameters. Composites: Part A 2010; 41(3): 391-400.

6. Durão Luís Miguel P, Gonçalves Daniel J.S, Tavares João Manuel R.S, de Albuquerque Victor Hugo C., Aguiar Vieira A., Torres Marques A. Drilling tool geometry evaluation for reinforced composite laminates. Composite Structures 2010; 92 (7): 1545-1550.

7. Iliescu D, Gehin D, Gutierrez M.E, Girot F. Modeling and tool wear in drilling of CFRP. International Journal of Machine Tools and Manufacture 2010; 50(2): 204–213.

8. Abe Y, Kato T, Mori K. Self-piercing riveting of high tensile strength steel and aluminium alloy sheets using conventional rivet and die. Journal of Materials Processing Technology 2008; 209(8): 3914-3922.

9. Hoang NH, Porcaro R, Langseth M, Hanssen AG. Self-piercing riveting connections using aluminium rivets. International Journal of Solids and Structure 2010; 47(3-4): 427-439.

10. McCarthy MA, Lawlor VP, Stanley WF, McCarthy CT. Bolt-hole clearance effects and strength criteria in single bolt, single lap, composite joints. Composites Science and Technology 2002; 62(10-11): 1415-1431.

11. Stockdale J.H., Matthews F.L. The effect of clamping pressure on bolt bearing loads in glass fibre-reinforced plastics. Composites 1976; 7(1): 34-38.

12. Collings TA. The strength of bolted joints in multi-directional CFRP laminates. Composites 1977; 8(1): 43-54.

13. Kretsis G, Matthews FL. The strength of bolted joints in glass fibre/epoxy laminates. Composites 1985; 16(2): 2-105.

14. Valenza A., Fiore V. Failure map of composite laminate mechanical joint. Journal of Composite Materials 2007; 41(8): 951-964.
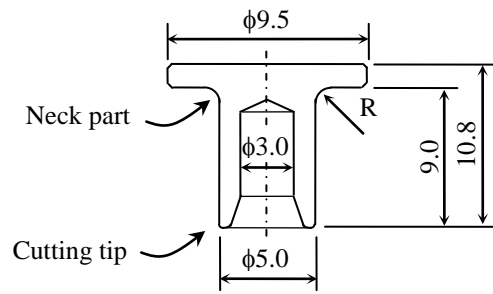
(a) Rivet body
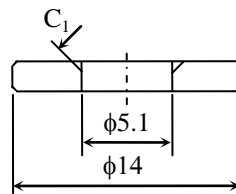
(b) Upper flat washer
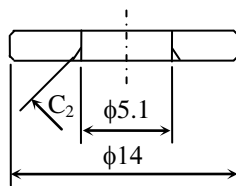
(c) Lower flat washer

Fig.1 Configuration of modified SPR

(3) Upper supporting die

(1) Upper flat washer

Pressure

← Upper CFRP laminate
← Lower CFRP laminate

(2) Lower flat washer

(4) Lower supporting die

Pressure

(a) Before joining

(b) After joining
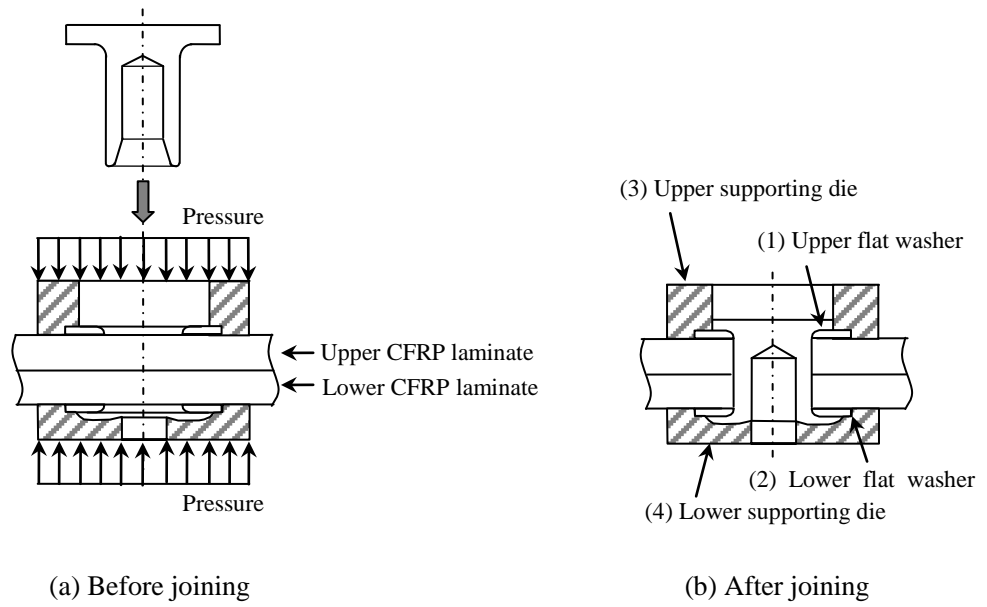
Fig.2 Joining of CFRP laminates by modified SPR

Piercing of CFRP

(a) Piercing process

Swaging of cutting tip
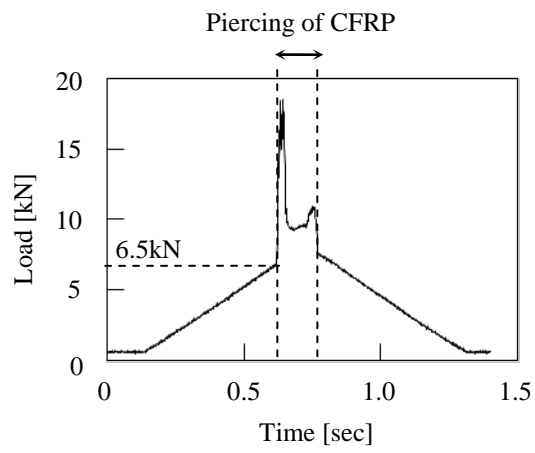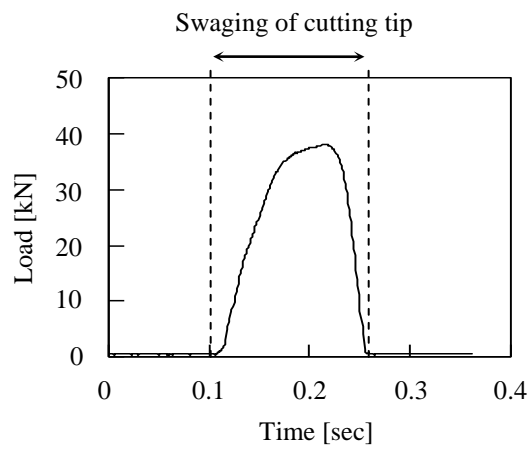
(b) Swaging process

Fig. 3 Load-time curves in the fastening process

Rivet body

Upper flat washer

Upper CFRP laminate

Lower CFRP laminate

Lower flat washer

Curled part

Dragging
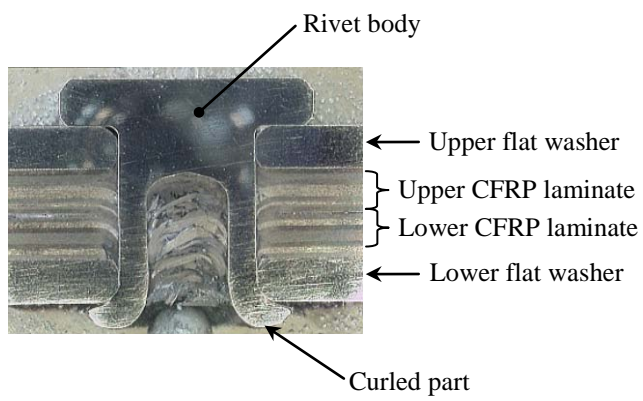
(a) Photograph
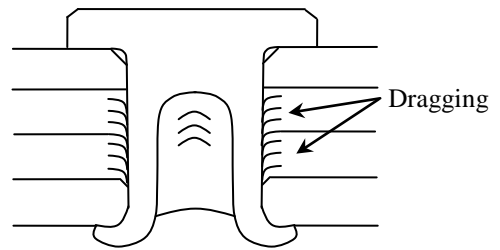
(b) Schematic drawing

Fig.4 Cross-section of jointed CFRP laminate by modified SPR

Outer diameter of flat washer
Piercing hole

(i) C-scan image   (ii) Specimen surface (piercing side)

(a) Upper laminate

Outer diameter of flat washer
Piercing hole

(i) C-scan image   (ii) Specimen surface (curling side)

(b) Lower laminate
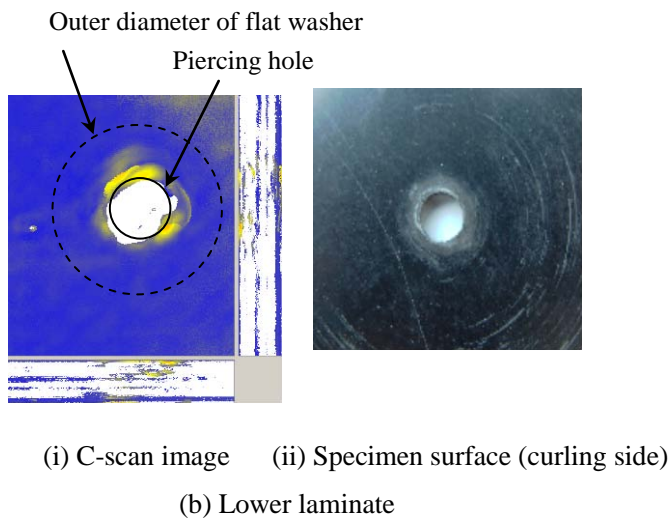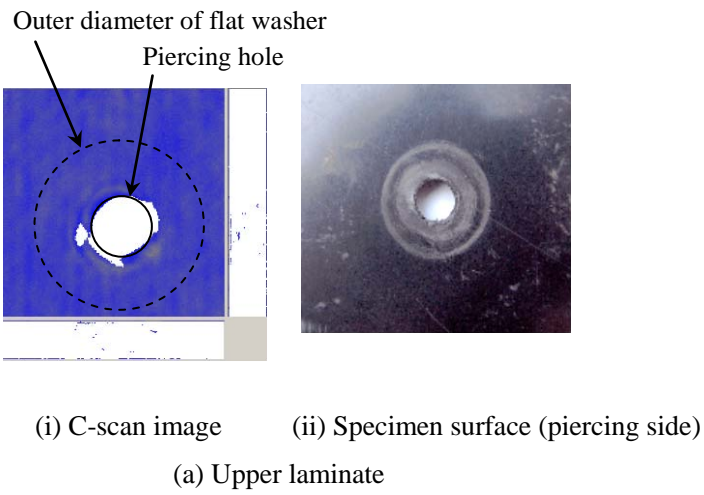
Fig.5 C-Scan images of delaminations in quasi-isotropic CFRP laminates and external appearances after piercing
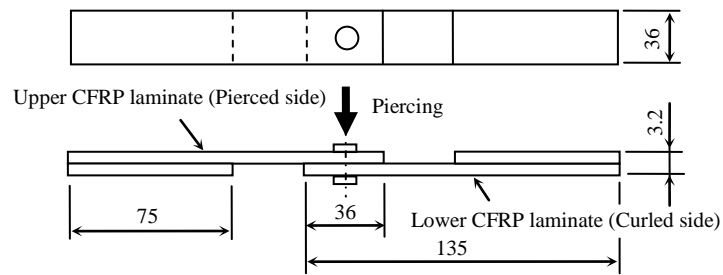
(a) Configuration of single lap joint
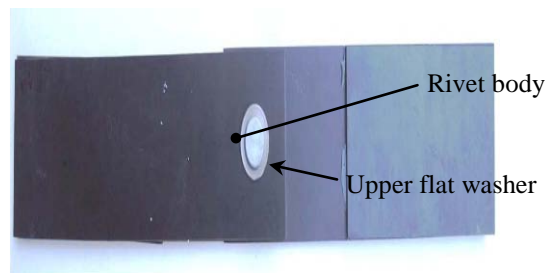
(b) Front view
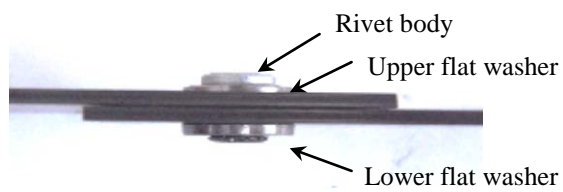
(c) Side view

Fig.6 CFRP laminates jointed by modified SPR
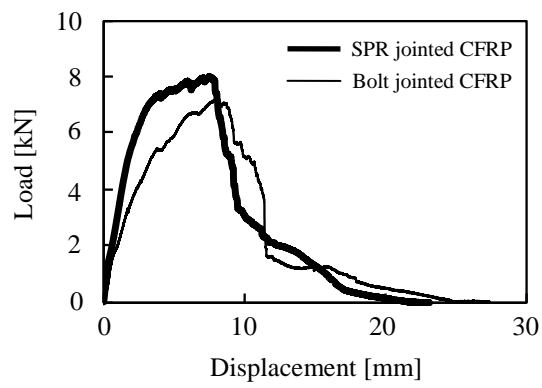
Fig.7 Load-displacement curves of joints

<div align="center">
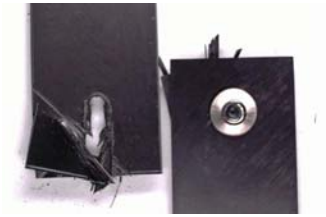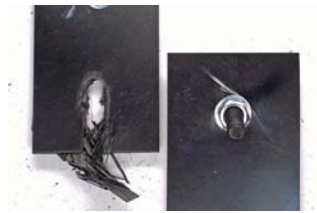
(a) Modified SPR joint   (b) Bolted joint

Fig.8 Final failure of joints after tensile tests

</div>
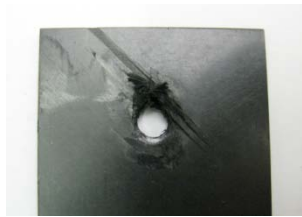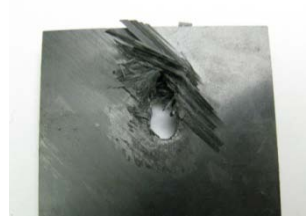
(a) Bearing failure   (b) Progressive damage after bearing failure

Fig. 9 Bearing failure of modified SPR joint

□ : Failure of CFRP   ○ : Failure of rivet
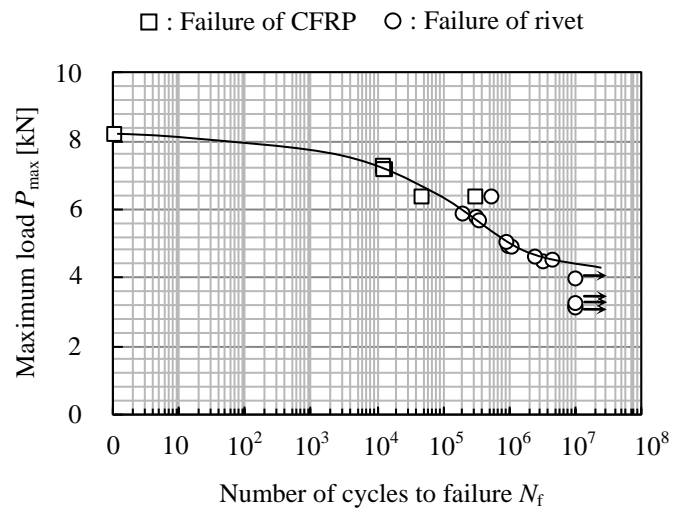
Fig.10 Maximum load-cycles to failure curve of CFRP laminates jointed by modified SPR
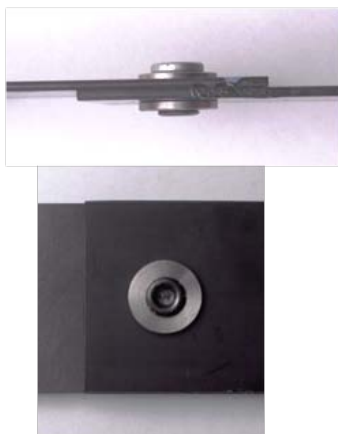
Fig.11 Modified SPR joint after fatigue test
(P_{max}=0.5P_{U}, N_{f}=10^7)

—— Piercing hole

- - - - - Outer diameter of flat washer
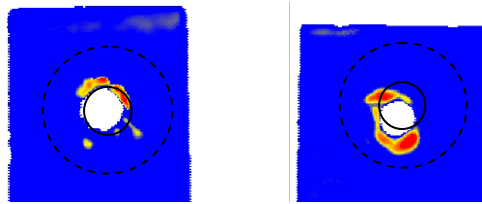
(a) Upper CFRP laminate　　(b) Lower CFRP laminate

Fig.12 C-scan images of CFRP laminates after fatigue test

$(P_{max}=0.5P_{U}, N_{f}=10^{7})$

——— Piercing hole

- - - - - Outer diameter of flat washer
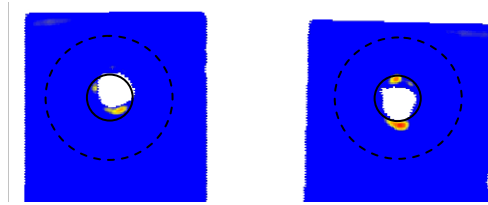
(a) Upper CFRP laminate   (b) Lower CFRP laminate

Fig.13 C-scan images of CFRP laminates after fatigue test

$(P_{max}=0.4P_{U}, N_f=10^7)$